Radiology: Cardiothoracic Imaging

Chest CT Findings in Cases from the Cruise Ship "Diamond Princess" with Coronavirus Disease 2019 (COVID-19)

Shohei Inui, MD[1, 2, *]; Akira Fujikawa, MD, PhD[1]; Motoyuki Jitsu, MD[1]; Naoaki Kunishima, MD, PhD[1]; Sadahiro Watanabe, MD, PhD[1]; Yuhi Suzuki, MD[1]; Satoshi Umeda, MD[1]; Yasuhide Uwabe, MD, PhD[3]

1. Department of Radiology, Japan Self-Defense Forces Central Hospital, 1-2-24, Ikejiri, Setagaya-ku, Tokyo, 154-0001, Japan
2. Department of Radiology, Graduate School of Medicine, The University of Tokyo, 7-3-1, Hongo, Bunkyo-ku, Tokyo, 113-0033, Japan
3. Department of Respiratory Medicine, Japan Self-Defense Forces Central Hospital, Tokyo, 1-2-24, Ikejiri, Setagaya-ku, Tokyo, 154-0001, Japan

*Corresponding author

Correspondence to:

Shohei Inui, MD

1. Department of Radiology, Japan Self-Defense Force Central Hospital

1-2-24, Ikejiri, Setagaya-ku, Tokyo, 154-0001, Japan

2. Department of Radiology, Graduate School of Medicine, The University of Tokyo

7-3-1, Hongo, Bunkyo-ku, Tokyo, 113-0033, Japan

Email: shohei.inui.ndmc@gmail.com

Funding:

No funding is provided in this study.

Disclosure of Conflicts of Interest:

No financial conflicts of interest to disclose with regard to this study.

Keywords:

Coronavirus Disease 2019, COVID-19, Japan, Diamond Princess, CT

Abbreviations:

Coronavirus: CoV

World Health Organization: WHO

RT-PCR: real-time reverse transcription polymerase chain reaction

CT: computed tomography

Ground-glass opacity: GGO

Key Points:

・Of 112 cases analyzed, 82 (73%) were asymptomatic, 44 (54%) of which had pneumonic changes on CT. Other 30 (27%) cases were symptomatic, 24 (80%) of which had abnormal CT findings.

・Asymptomatic cases showed more GGO predominance over consolidation (80%), while symptomatic cases were more likely to show a consolidation predominance over GGO (38%).

・Asymptomatic cases showed milder CT severity score than symptomatic cases.

Summary statement:

We revealed a high incidence of subclinical CT changes in COVID-19 infected cases, which showed more GGO predominance over consolidation and milder severity on CT than symptomatic cases.

Chest CT Findings in Cases from the Cruise Ship "Diamond Princess" with Coronavirus Disease 2019 (COVID-19)

Abstract

Purpose: To evaluate the chest CT findings in an environmentally homogeneous cohort from the cruise ship "Diamond Princess" with Coronavirus Disease 2019 (COVID-19).

Materials and Methods: This retrospective study comprised 112 cases (mean age, 62 years ± 16, range 25-93) with COVID-19 confirmed with RT-PCR. CT images were reviewed and the CT severity score was calculated for each lobes and the entire lung. CT findings were compared between asymptomatic and symptomatic cases.

Results: Of 112 cases, 82 (73%) were asymptomatic, 44 (54%) of which had lung opacities on CT. Other 30 (27%) cases were symptomatic, 24 (80%) of which had abnormal CT findings. Symptomatic cases showed lung opacities and airway abnormalities on CT more frequently than asymptomatic cases [lung opacity; 24 (80%) vs 44 (54%), airway abnormalities; 15 (50%) vs 15 (18%)]. Asymptomatic cases showed more GGO over consolidation (80%), while symptomatic cases more frequently showed consolidation over GGO (38%). The CT severity score was higher in symptomatic cases than asymptomatic cases, particularly in the lower lobes [symptomatic vs asymptomatic cases; right lower lobe: 2 ± 1 (0-4) vs 1 ± 1 (0-4); left lower lobe: 2 ± 1 (0-3) vs 1 ± 1 (0-3); total score: 7 ± 4 (1-17) vs 4 ± 2 (1-11)].

Conclusion: This study documented a high incidence of subclinical CT changes in cases with COVID-19. Compared to symptomatic cases, asymptomatic cases showed more GGO over consolidation and milder extension of disease on CT.

Introduction

The respiratory infection caused by a new strain of coronavirus not previously identified in humans, SARS-CoV-2, has received the name of Coronavirus Disease 2019, COVID-19 (1). Originally reported in December 2019 as “pneumonia of unknown cause” in Wuhan City, Hubei Province, China, COVID-19 has spread rapidly and progressively to other regions of China as well as adjacent Asian countries (2). The International Health Regulations Emergency Committee of the World Health Organization officially declared the outbreak a “public health emergency of international concern” on January 30, 2020, and the disease was declared pandemic on March 11, 2020.

Recently, the international cruise ship “Diamond Princess”, carrying about 3,700 passengers, temporarily became the largest cluster of COVID-19 cases outside China (3). The cruise ship docked at Yokohama Bay, Japan, on February 3, 2020, and after quarantine, passengers started to disembark on February 14, 2020. The Ministry of Health, Labor, and Welfare from Japan reported that of the 1,723 national passengers, a cumulative number of 454 cases were recognized as pathogen carriers on real-time reverse transcription polymerase chain reaction (RT-PCR), including 189 asymptomatic cases who initially tested negative on February 17, 2020. During and after the quarantine period, passengers and crew members were referred to the Japan Self-Defense Forces Central Hospital by the government.

The clinical course and spectrum of radiological patterns seen in COVID-19 have gradually become apparent with recent publications; however, most publications have been focused on symptomatic cases occurring in China (9, 13, 15-19). This prompted us to undertake the present study to retrospectively evaluate the computed tomographic (CT) findings in laboratory-confirmed cases of COVID-19, conveniently sampled from the passengers and crew members of the “Diamond Princess” cruise ship in Japan. We specifically compared the radiological findings of COVID-19 infection between asymptomatic and symptomatic cases.

Materials and Methods

Cases

This study was approved by the Institutional ethics review board, and written informed consent was obtained from all cases. In this retrospective study, the medical records were reviewed for clinical and imaging findings of cases diagnosed with COVID-19 from February 7th to 28th, 2020. Passengers and crew members of the "Diamond Princess" cruise ship underwent RT-PCR during the quarantine period, and those who showed positive results were transferred to hospitals in Japan. Among all RT-PCR positive cases from the cruise ship, asymptomatic, mildly symptomatic, or familial clusters with infection among relatives were admitted to the Japan Self-Defense Forces Central Hospital (Tokyo, Japan) for further investigation. Consecutive cases from this single-center cohort who had confirmed COVID-19 infection and underwent chest CT were included. Those who showed negative results on RT-PCR underwent repeat RT-PCR examination. On admission, all cases underwent chest CT irrespective of the RT-PCR results, based on the following grounds: (1) a previous report describing positive CT findings in cases with RT-PCR positive status without symptoms (4, 5), (2) previous reports of person-to-person transmission from asymptomatic cases (6-8), and (3) the need to judge the precaution level necessary on admission to prevent nosocomial infection in the hospital. Based on our previous experience, CT parameters were optimized to minimize patient exposure to radiation as detailed below.

Clinical Data

The following data were extracted from the medical records: demographic data, medical history, presence or absence of underlying comorbidities, symptoms, and signs. Cases were classified as *symptomatic* if they had any signs or symptoms of pneumonia, including fever (>37.5℃), cough, dyspnea, and fatigue on admission. Otherwise, cases were classified as *asymptomatic*.

Chest CT Acquisition

Non-enhanced chest CT was performed using a 6-row multi-detector CT unit (SOMATOM Emotion 6 scanner; Siemens, Tokyo, Japan) on admission with the following parameters: tube

voltage, 130 kVp; effective current 95 mA; collimation, 6×2 mm, helical pitch, 1.4. Acquisition parameters were modified to minimize patient radiation exposure while maintaining sufficient resolution for chest CT evaluation. Based on measurements of the dosimetry phantom (diameter 32 cm, length 35 cm) under automatic exposure control (CARE Dose4D; Siemens, Tokyo, Japan), the radiation exposure of each subject was estimated to be less than 2.8 mSv. CT images were acquired during a single inspiratory breath-hold to minimize motion artifacts. A 2.0-mm gapless section was reconstructed before being reviewed on the picture archiving and communication system (PACS) monitor.

Image Analysis

Image analysis was performed independently by three chest radiologists (A. F., M. J., and S.I. with 31, 19 and 6 years of experience, respectively), who were blinded to the clinical data, followed by joint consensus. The chest CT findings were recorded based on the Fleischner Society glossary of terms (9-12). Parameters evaluated included: the presence or absence of ground-glass opacity (GGO), consolidation, intra- or interlobular septal thickening, linear opacities (including subpleural curvilinear opacities), and "reversed halo" sign. According to the proportion of each pattern in comparison with the totality of the lung opacification, cases were classified as *GGO dominant* or *consolidation dominant*, if the proportion of each one of the patterns was respectively greater than 50% of the total (13). Zonal distribution patterns of the lesion were visually classified as peripheral predominant (involving mainly the peripheral one-third of the lung), central or peribronchovascular predominant, or mixed (without predilection for subpleural or central region) (14).

The number of lobes involved and laterality of lung abnormalities were determined. A semi-quantitative scoring system was used to quantitatively estimate the pulmonary involvement of all these abnormalities on the basis of the percentage of the total lung involved per lobe (9, 15). The extension of the lung opacification was visually scored from 0 to 5 as follows: score 1, 1-5% involvement; score 2, 6-25% involvement; score 3; 26-50% involvement; score 4, 51-75%

involvement; score 5, 76-100% involvement. Total lung scores were calculated as the sum of individual lobe scores.

The presence or absence of pleural effusion, thoracic lymphadenopathy (as defined by lymph node size of ≥ 10mm in short-axis dimension), airway abnormalities (i.e. airway wall thickening, bronchiectasis, and endoluminal secretions), and any underlying lung disease, including emphysema or fibrosis was also recorded.

Statistics

Statistical analysis was done using the SPSS 11.0 statistical software program (Dr. SPSS II for Windows, standard version 11.0; SPSS Inc, Chicago, IL, USA). Quantitative variables were expressed as mean±standard deviation (range), and the categorical variables were presented as the percentage of the total. The comparisons of categorical data were evaluated using Pearson $\chi 2$ test and non-paired quantitative data using the Mann-Whitney U test, according to the normal distribution assessed by the Shapiro-Wilk test. Statistical significance level was set at $p < 0.05$.

Results

Clinical Findings

Demographics and clinical characteristics of the study population are summarized in **Table 1**. The study population comprised 112 cases (59 men, mean age, 60 years ± 17, range: 31-87; 53 women, 63 years ± 15, range: 25-93). Of these cases, 82 (73%) were asymptomatic and 30 (27%) cases were symptomatic. The most frequent symptoms on admission were cough (21 [19%] cases), fever (11 [10%] cases), and fatigue (11 [10%] cases).

Chest CT Findings

The frequencies of the major chest CT findings of all cases are summarized in **Table 2**. Abnormal lung opacities (GGO and/or consolidation) and airway abnormalities (bronchiectasis and/or

bronchial wall thickening) were present in 68 (61%) and 30 (27%) of the whole cohort, respectively. Lung opacities on CT were found in 44 (54%) of 82 asymptomatic. Twenty-four (80%) of 30 symptomatic cases had abnormal CT findings consistent with viral pneumonia. Comparing the two groups, symptomatic cases showed lung parenchymal and airway abnormalities on CT more frequently than did asymptomatic cases [symptomatic vs asymptomatic, lung opacity: 24 (80%) vs 44 (54%), p=0.012; airway lesion: 15 (50%) vs 15 (18%), p<0.001]. No significant differences in age, sex distribution, or comorbidities were identified between symptomatic and asymptomatic cases. Representative CT patterns of asymptomatic cases are shown in **Figures 1-3**.

CT patterns were compared between asymptomatic and symptomatic cases who had positive lung parenchymal CT findings. The results are summarized in **Table 3**. Of 44 asymptomatic cases with lung opacities on CT, 18 (41%) cases had pure GGO, 7 (16%) GGO with intra- and interlobular septal thickening without consolidation, and 19 (43%) GGO with consolidation. Of 24 symptomatic cases who had lung opacities on CT, 7 (29%) cases had pure GGO, 4 (17%) GGO with intra- and interlobular septal thickening and without consolidation and 13 (54%) GGO with consolidation. In terms of the predominance of the lung parenchymal findings, asymptomatic cases showed GGO predominance over consolidation, while symptomatic cases were more likely to show consolidation predominance over GGO [asymptomatic vs symptomatic cases; GGO predominance: 35 (80%) vs 15 (63%); consolidation predominance: 9 (20%) vs 9 (38%), p<0.001]. In terms of the number of lesions, asymptomatic cases had a single lesion in 11 (25%) and more than 2 in 33 (75%) cases, compared to symptomatic cases, who had a single lesion in 5 (21%) and more than 2 in 19 (79%) cases. In terms of the axial distribution, more than half of the cases in each group showed a peripheral dominant distribution [25 (57%) asymptomatic vs 13 (54%) symptomatic cases]. On the other hand, only asymptomatic cases [5 (11%) cases] showed a central dominant distribution with single or multiple rounded GGO in one

or multiple lobes. Symptomatic cases were more likely to show a mixed distribution (coexisting peripheral and central distribution) than asymptomatic cases [11 (46%) symptomatic vs 14 (32%) asymptomatic cases]. In both groups, the lower lobes were the most frequently affected; left and right lower lobe involvement was present in 18 (75%) of symptomatic cases and 32 (73%) of asymptomatic cases. In addition, more than 2 lung lobes were affected in more than 75% of cases and bilateral lungs in more than 80% in both clinical groups. The CT severity score was significantly higher in symptomatic cases than asymptomatic cases in the right and left lower lobes and overall lung [symptomatic vs asymptomatic cases; right lower lobe: 2 ± 1 (0-4) vs 1 ± 1 (0-4), p=0.047; left lower lobe: 2 ± 1 (0-3) vs 1 ± 1 (0-3), p=0.032; total lung score: 7 ± 4 (1-17) vs 4 ± 2 (1-11), p=0.015].

Airway abnormalities included dilated bronchi in association with GGO or consolidation (i.e., as "air bronchograms"), without airway secretions. Cavitation, thoracic lymphadenopathy and pleural effusion were not observed.

Discussion

In this study, we investigated the chest CT findings in laboratory-confirmed COVID-19 cases in an environmentally homogenous cohort of cruise ship passengers and crew members, comparing the CT characteristics of asymptomatic and symptomatic cases. Although lung parenchymal and airway abnormalities were more frequent in symptomatically than asymptomatic cases, noticeably, we found lung parenchymal changes on CT in up to 54% of the asymptomatic cases. In those who showed CT abnormalities, asymptomatic cases showed significantly predominance of GGO, while consolidation was predominant in symptomatic cases. Similarly, the CT severity score was significantly higher in symptomatic cases than asymptomatic cases in both lower lobes and on total lung assessment.

Although various CT findings were observed in cases with COVID-19, we found several

common characteristic CT patterns, such as (1) single or multiple half-round or rectangular-shaped GGO in subpleural area with or without intra- or interlobular septal thickening (Figure 1), (2) single or multiple rounded GGO in both peribronchial and subpleural areas (Figure 2), (3) bilateral diffuse or multiple patchy GGO with or without intra- or interlobular septal thickening or consolidation in both peribronchial and subpleural areas, with a lower lobe predilection (Figure3). Dilated bronchi were frequently associated with all of these CT patterns. These observations are mostly consistent with those of previous studies from China (9, 13, 15-19). All of the above-described characteristic CT patterns were found in both groups. However, differences were observed in the extension of the lung involvement as calculated by the mean CT severity score. The maximum total lung CT score was 11 in asymptomatic cases and 17 in symptomatic cases. In addition, the predominance of opacities also differed between the two groups; GGO was predominant in asymptomatic cases, whereas consolidation was predominant in symptomatic cases.

Some studies have reported clinical-radiological dissociation in COVID-19 (20). For instance, several previous reports described asymptomatic cases who had evidence of lung opacities on chest CT (4, 5, 13). These observations have been confirmed by the results of the present study, highlighting the relative high prevalence of CT abnormalities even in asymptomatic cases. The presence of the subclinical CT findings in COVID-19 is an enigma. To the best of our knowledge, such cases with subclinical CT abnormalities have not been reported in either Middle East Respiratory Syndrome (MERS-CoV) or Severe Acute Respiratory Syndrome (SARS-Cov) infection. Several hypotheses could explain this discrepancy. One possibility is that these cases have developed immunity against SARS-CoV-2 due to re-infection, leading to subclinical presentation. Such a case of relapse was reported from China and a suspected case of re-infection from Japan (21, 22). Other possibilities are that such cases are still in the healing phase of COVID-19, and the symptoms may have already subsided by the time of admission and CT scan. However, the lack of typical characteristic of the healing stage of COVID-19 pneumonia have not been frequently observed (e.g., perilobular pattern), weakening this hypothesis (9, 19). Other

possibilities include a discrepancy between the timing of CT positivity and clinical symptoms like in other types of pneumonia. The clinical-radiological dissociation noted in many of COVID-19 cases in this cohort is a conundrum that still needs further investigation.

RT-PCR is currently considered as the gold standard diagnostic method for COVID-19. However, the sensitivity of this method in throat swabs in COVID-19 is around 59% (23). To date, in several studies the sensitivity of chest CT has exceeded that of RT-PCR, and the authors emphasized the potential of chest CT as the primary screening tool for COVID-19 (24, 25). The sensitivity of chest CT is unquestionable and encouraged for cases where there is need to determine the extension of disease and alternative diagnoses. The results of this study, however, do not directly allow the conclusion that all persons with positive RT-PCR findings should undergo chest CT for screening purposes. Before arriving at any such conclusion, the bioactivity and clinical impact of asymptomatic CT findings in COVID-19 infection will have to be investigated. One important issue is the need to distinguish the natural history of symptomatic and asymptomatic COVID-19 cases presenting with CT abnormalities, including the potential for infectivity and progression to acute severe respiratory distress. More appropriate use of CT will be possible when this information becomes available.

This study has various limitations. First, it included only adult cases. Second, because it included only passengers and crew members of a cruise ship, we acknowledge a selection bias. However, this environmentally homogeneous cohort enabled an investigation that eliminates other potential geographic confounders.

In conclusion, this study documented a high incidence of subclinical CT changes in COVID-19. Asymptomatic cases showed more GGO over consolidation and milder extension of lung parenchymal opacities. Further studies still are warranted to uncover the underlying mechanism responsible for the clinical-radiological dissociation seen in some of asymptomatic COVID-19 cases, as well as to determine the impact of this findings on clinical decision-making.

References

1. https://www.who.int/emergencies/diseases/novel-coronavirus-2019/technical-guidance/naming-the-coronavirus-disease-(covid-2019)-and-the-virus-that-causes-it (accessed on 03/05/2020).
2. Huang C, Wang Y, Li X, et al. Clinical features of cases infected with 2019 novel coronavirus in Wuhan, China. The Lancet. 2020;395(10223):497-506.
3. The Ministry of Health LaW. The infection control measures taken at the Cruise ship "Diamond Princess"（provisional translation. https://www.mhlw.go.jp/stf/seisakunitsuite/newpage_00001.html
4. Shi H, Han X, Jiang N, et al. Radiological findings from 81 patients with COVID-19 pneumonia in Wuhan, China: a descriptive study. The Lancet Infectious Diseases. 2020. DOI: 10.1016/S1473-3099(20)30086-4.
5. Chung M, Bernheim A, Mei X, et al. CT imaging features of 2019 novel coronavirus (2019-nCoV). Radiology. 2020:200230.
6. Yu P, Zhu J, Zhang Z, et al. A familial cluster of infection associated with the 2019 novel coronavirus indicating potential person-to-person transmission during the incubation period. The Journal of Infectious Diseases. 2020.
7. Rothe C, Schunk M, Sothmann P, et al. Transmission of 2019-nCoV infection from an asymptomatic contact in Germany. New England Journal of Medicine. 2020.
8. Bai Y, Yao L, Wei T, et al. Presumed Asymptomatic Carrier Transmission of COVID-19. JAMA. 2020.
9. Pan F, Ye T, Sun P, et al. Time course of lung changes on chest CT during recovery from 2019 novel coronavirus (COVID-19) pneumonia. Radiology. 2020:200370.
10. Koo HJ, Lim S, Choe J, et al. Radiographic and CT features of viral pneumonia. Radiographics. 2018;38(3):719-39.
11. Hansell DM, Bankier AA, MacMahon H, et al. Fleischner Society: glossary of terms for thoracic imaging. Radiology. 2008;246(3):697-722.
12. Chang Y-C, Yu C-J, Chang S-C, et al. Pulmonary sequelae in convalescent cases after severe acute respiratory syndrome: evaluation with thin-section CT. Radiology. 2005;236(3):1067-75.
13. Ng M-Y, Lee EY, Yang J, et al. Imaging profile of the COVID-19 infection: radiologic findings and literature review. Radiology: Cardiothoracic Imaging. 2020;2(1):e200034.
14. Kanne JP. Chest CT findings in 2019 novel coronavirus (2019-nCoV) infections from Wuhan, China: key points for the radiologist. Radiology. 2020:200241.
15. Bernheim A, Mei X, Huang M, et al. Chest CT Findings in Coronavirus Disease-19 (COVID-19): Relationship to Duration of Infection. Radiology. 2020:200463.
16. Zu ZY, Jiang MD, Xu PP, et al. Coronavirus Disease 2019 (COVID-19): A Perspective from China. Radiology. 2020:200490.

17. Song F, Shi N, Shan F, et al. Emerging coronavirus 2019-nCoV pneumonia. Radiology. 2020:200274.

18. Pan Y, Guan H, Zhou S, et al. Initial CT findings and temporal changes in cases with the novel coronavirus pneumonia (2019-nCoV): a study of 63 cases in Wuhan, China. European Radiology. 2020:1-4.

19. Kong W, Agarwal PP. Chest imaging appearance of COVID-19 infection. Radiology: Cardiothoracic Imaging. 2020;2(1):e200028.

20. Chan J, Yuan S, Kok K, et al. Poon 20 RW, Tsoi HW, Lo SK, Chan KH, et al. A familial cluster of pneumonia associated 21 with the 2019 novel coronavirus indicating person-to-person transmission: a 22 study of a family cluster. Lancet. 2020;23.

21. D Chen, W Xu, Z Lei, et al. Recurrence of positive SARS-CoV2 RNA in COVID-19: A case report. International Journal of Infectious Diseases. 2020.

22. Osaka Prefectural Government, Japan. http://www.pref.osaka.lg.jp.e.agb.hp.transer.com/hodo/index.php?site=fumin&pageId=37523

23. Ai T, Yang Z, Hou H, Zhan C, Chen C, Lv W, Tao Q, Sun Z, Xia L. Correlation of Chest CT and RT-PCR Testing in Coronavirus Disease 2019 (COVID-19) in China: A Report of 1014 Cases. Radiology. 2020 Feb 26:200642. doi: 10.1148/radiol.2020200642. [Epub ahead of print] PubMed PMID: 32101510.

24. Fang Y, Zhang H, Xie J, et al. Sensitivity of Chest CT for COVID-19: Comparison to RT-PCR. Radiology. 2020:200432.

25. Ai T, Yang Z, Hou H, et al. Correlation of Chest CT and RT-PCR Testing in Coronavirus Disease 2019 (COVID-19) in China: A Report of 1014 Cases. Radiology. 2020.

Table 1. Characteristics of the patient cohort.

Parameter	All Cases (N=112)
Gender	
Men	59 (53%)
Women	53 (47%)
Age (years)	62 ± 16 (25-93)
Symptoms on admission	
Fever	11 (10%)
Cough	21 (19%)
Sore throat	3 (3%)
Fatigue	11 (10%)
Dyspnea	4 (4%)
Nasal discharge	4 (4%)
Headache	5 (4%)
Diarrhea	3 (3%)

Note.-Data are number of cases. Percentage within parenthesis in comparison with all cases. Age, range within parenthesis.

Table 2. Frequency of lung abnormalities on CT

Parameter	All Cases (N=112)	Asymptomatic Cases (N=82)	Symptomatic Cases (N=30)	P-value
Lung opacities				
Present	68 (61%)	44 (54%)	24 (80%)	
Absent	44 (39%)	38 (46%)	6 (20%)	0.012
Airway abnormalities				
Present	30 (27%)	15 (18%)	15 (50%)	<0.001
Absent	82 (73%)	67 (82%)	15 (50%)	-
Underlying lung disease				
Emphysema	7 (6%)	4 (5%)	3 (10%)	N.S.
Pulmonary fibrosis	3 (3%)	2 (2%)	1 (3%)	N.S.
Other findings				
Cavitation	0 (0%)	0 (0%)	0 (0%)	-
Mediastinal lymphadenopathy	0 (0%)	0 (0%)	0 (0%)	-
Pleural effusion	0 (0%)	0 (0%)	0 (0%)	-

Note.-Data are number of cases. Abbreviations.—N.S.: not statistically significant.

Table 3. Summary of CT findings in cases with lung opacities.

Parameter	All Cases (N=68)	Asymptomatic Cases (N=44)	Symptomatic Cases (N=24)	P-value
Opacity frequency				
Pure GGO	25 (37%)	18 (41%)	7 (29%)	
Pure GGO with interlobular septal thickening	11 (16%)	7 (16%)	4 (17%)	
GGO+consolidation	32 (47%)	19 (43%)	13 (54%)	N.S.
Opacity predominance				
GGO > consolidation	50 (74%)	35 (80%)	15 (63%)	
Consolidation > GGO	18 (26%)	9 (20%)	9 (38%)	<0.001
Number of lesions				
<2	16 (24%)	11 (25%)	5 (21%)	
>2	52 (76%)	33 (75%)	19 (79%)	N.S.
Opacity distribution				
Peripheral distribution	38 (56%)	25 (57%)	13 (54%)	
Central distribution	5 (7%)	5 (11%)	0 (0%)	
Mixed distribution	25 (37%)	14 (32%)	11 (46%)	N.S.
Frequency of lobes affected				
Right upper lobe	33 (49%)	21 (48%)	12 (50%)	N.S.
Right middle lobe	26 (38%)	14 (32%)	12 (50%)	N.S.
Right lower lobe	49 (72%)	32 (73%)	17 (71%)	N.S.
Left upper lobe	38 (56%)	22 (50%)	16 (67%)	N.S.
Left lower lobe	47 (69%)	29 (66%)	18 (75%)	N.S.
Number of lobes affected				
1	16 (24%)	11 (25%)	5 (21%)	
2	18 (26%)	13 (30%)	5 (21%)	
3	10 (15%)	6 (14%)	4 (17%)	
4	9 (13%)	7 (16%)	2 (8%)	
5	15 (22%)	7 (16%)	8 (33%)	
More than 2 lobes affected	52 (76%)	33 (75%)	19 (79%)	N.S.
Bilateral lung involvement	56 (82%)	35 (80%)	21 (88%)	N.S.
Predominance				
Right lung	41 (60%)	29 (66%)	12 (50%)	
Left lung	27 (40%)	15 (34%)	12 (50%)	N.S.
Mean CT scores in each lobe				
Right upper lobe	2 ±1 (0-3)	1 ±1 (0-2)	1 ±1 (0-3)	N.S.
Right middle lobe	1 ±1 (0-3)	1 ±1 (0-3)	1 ±1 (0-3)	N.S.
Right lower lobe	2 ±1 (0-4)	1 ±1 (0-4)	2 ±1 (0-4)	0.047
Left upper lobe	2 ±1 (0-3)	1 ±1 (0-3)	1 ±1 (0-3)	N.S.
Left lower lobe	2 ±1 (0-3)	1 ±1 (0-3)	2 ±1 (0-3)	0.032
Total CT score	3 ±3 (1-17)	4 ±2 (1-11)	7 ±4 (1-17)	0.015

Note.—Data are number of cases. GGO, ground-glass opacities. Abbreviations.—N.S.: not statistically significant.

Figures

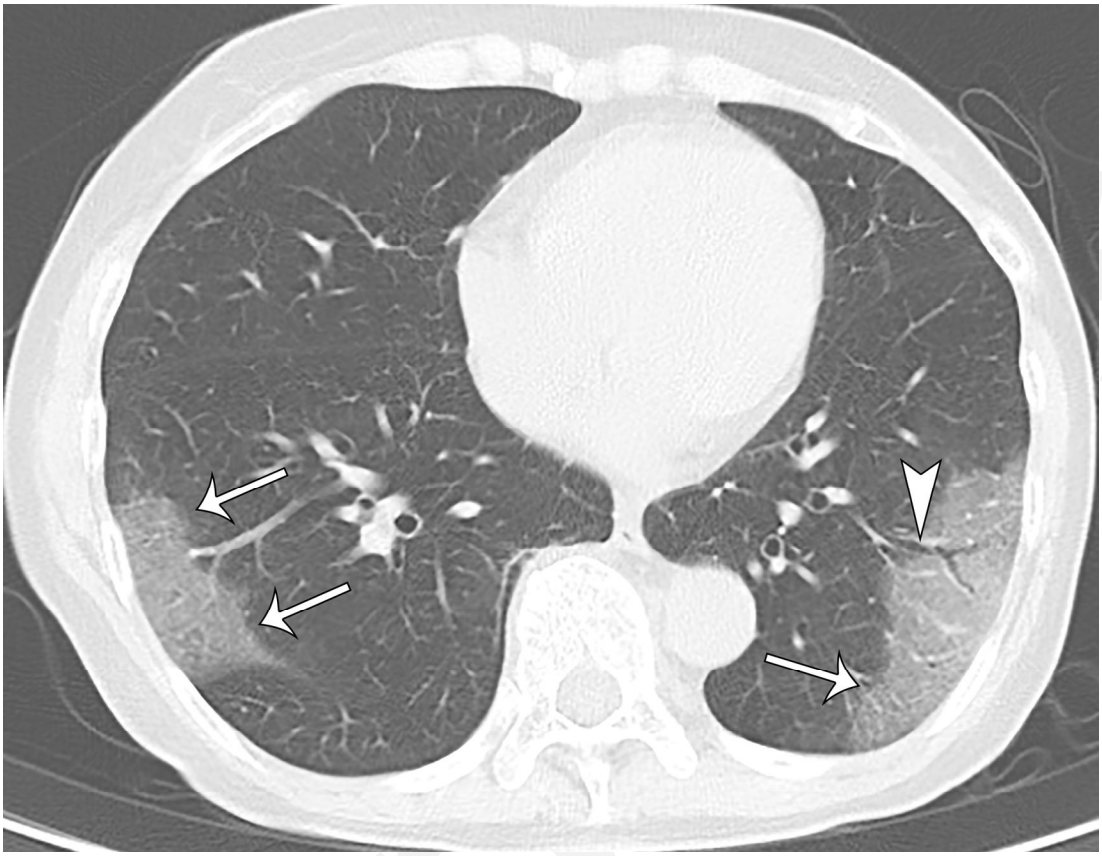

Figure 1. A 70-year-old asymptomatic woman. On axial CT image, focal subpleural ground-glass opacities with smooth intralobular and interlobular smooth septal thickening were demonstrated in the right and left lower lobes (arrow). The left lower lobe lesion was accompanied by air bronchogram with mild bronchial dilation (arrowhead).

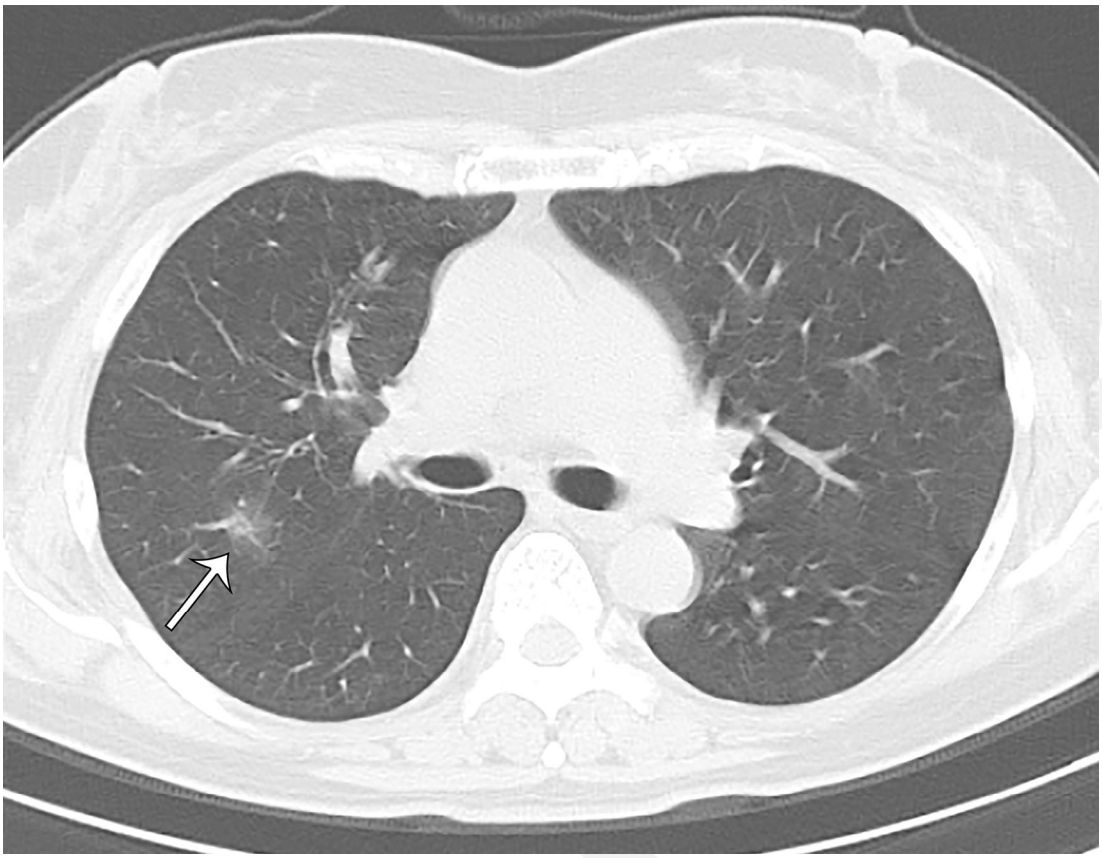

a.

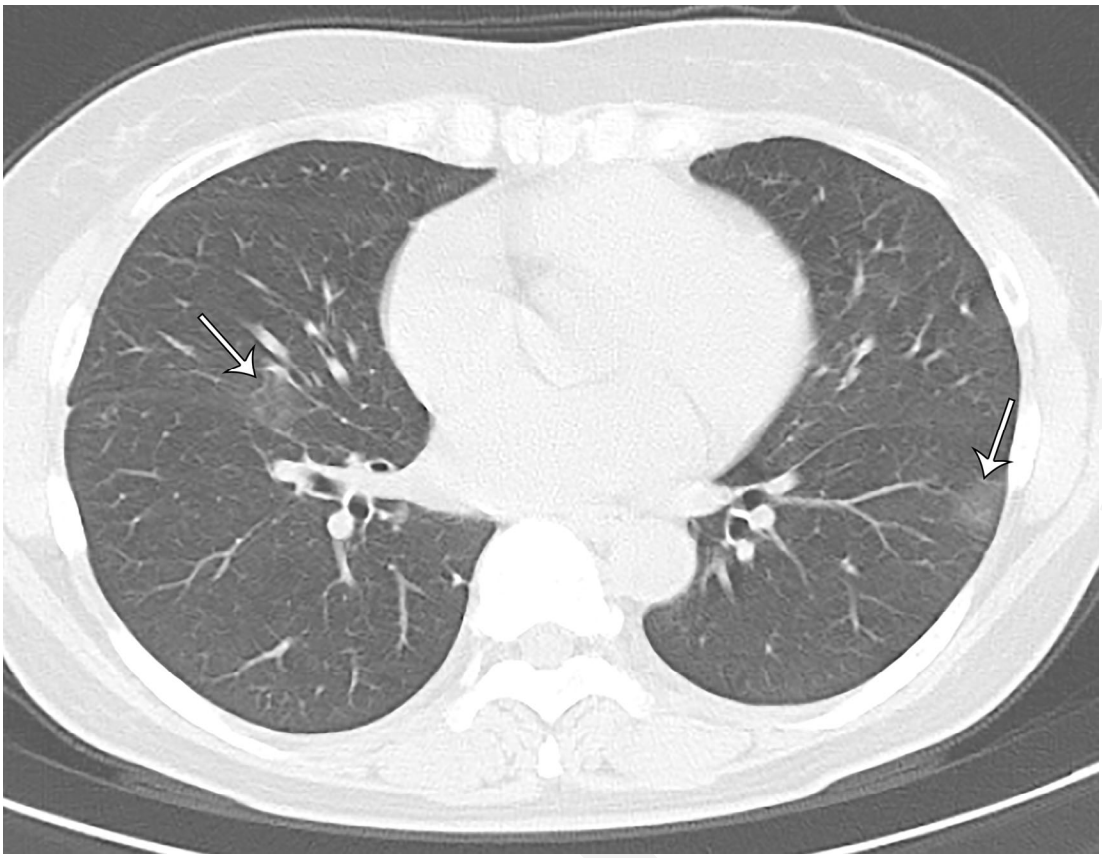

b.

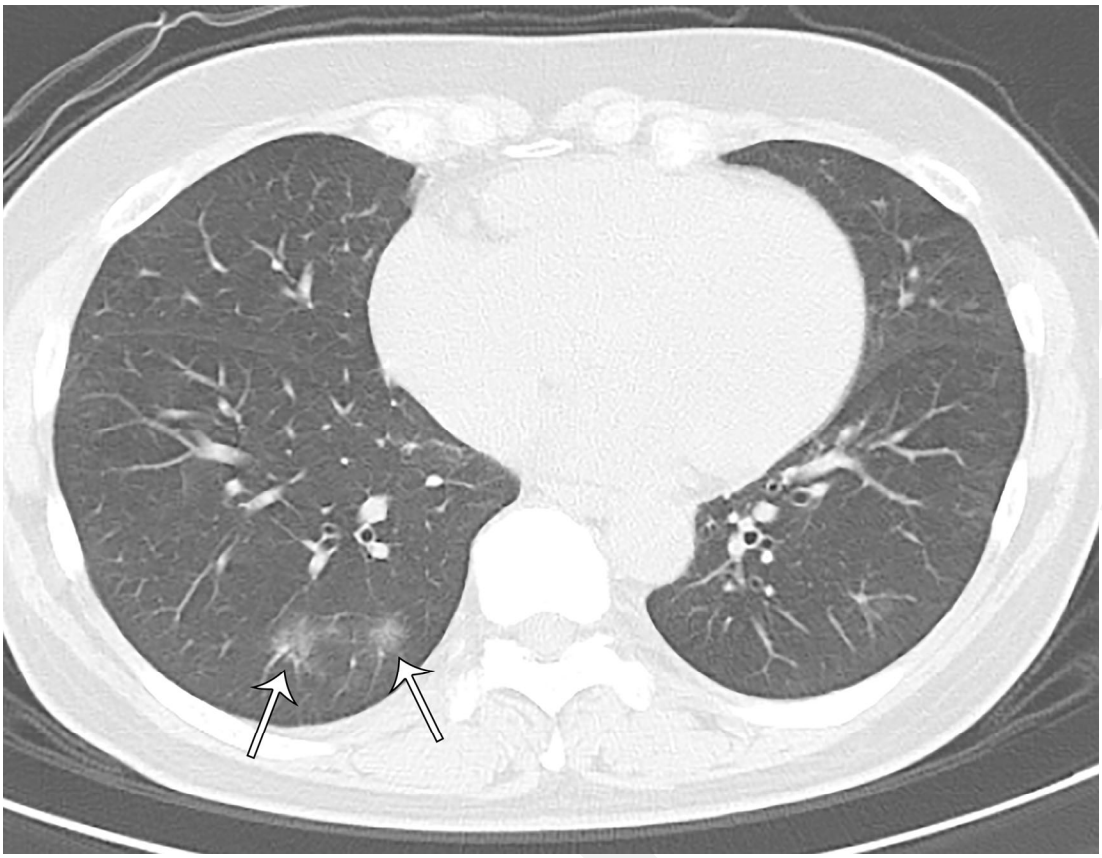

c.

Figure 2. A 66-year-old asymptomatic woman. On axial CT images, focal rounded ground-glass opacities with partial consolidation in a peribronchial and subpleural distribution were noted in the right upper (a), middle (b) and lower (c) and left lower (b) lobes.

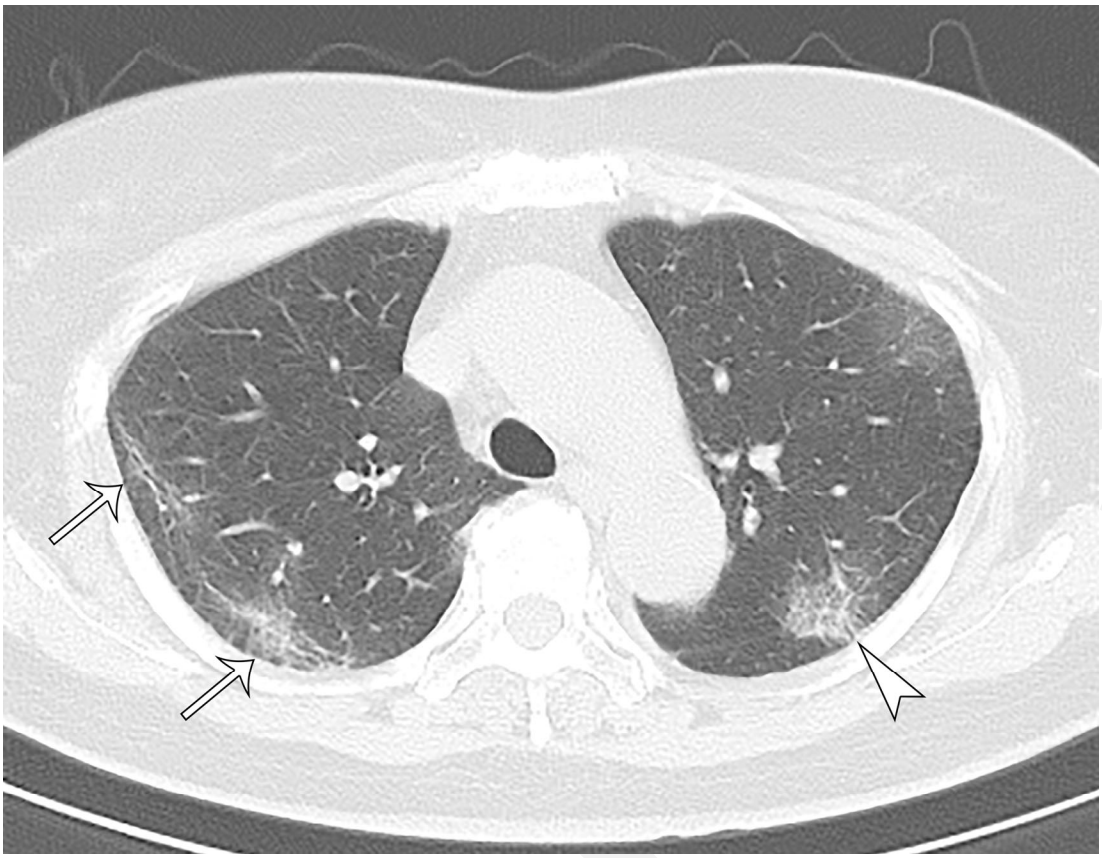

a.

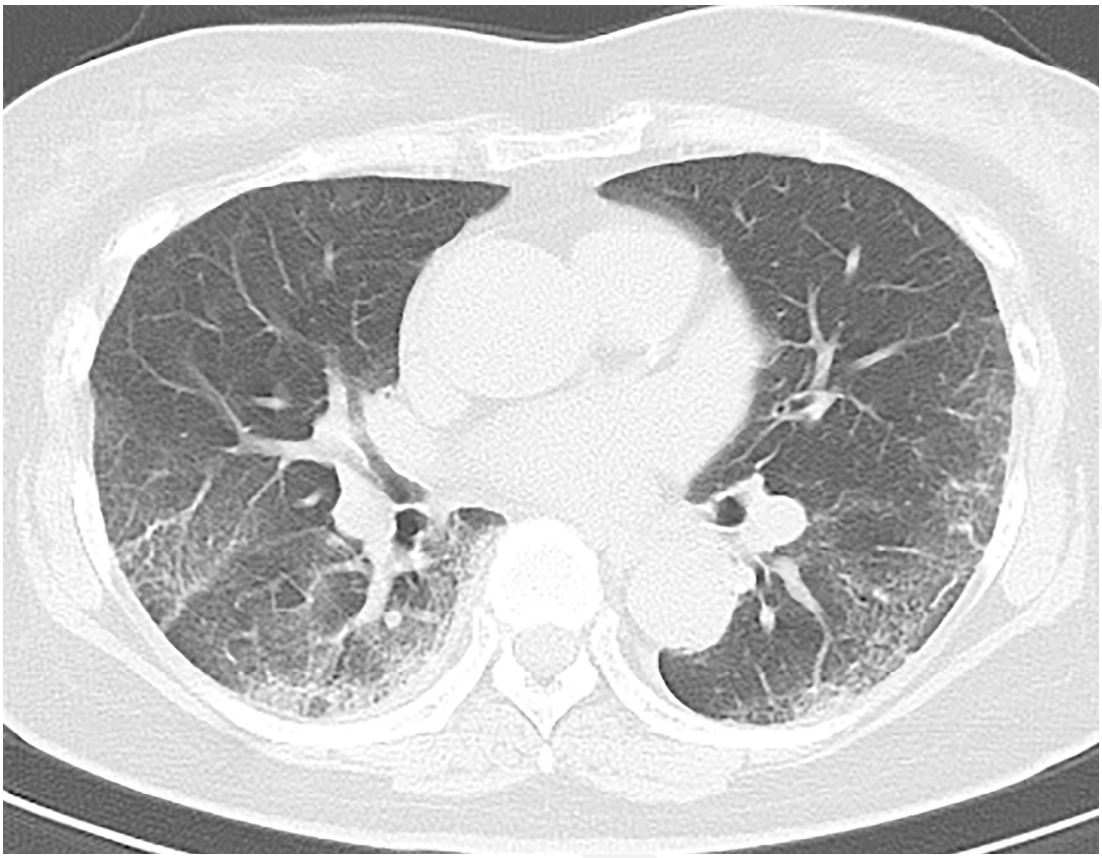

b.

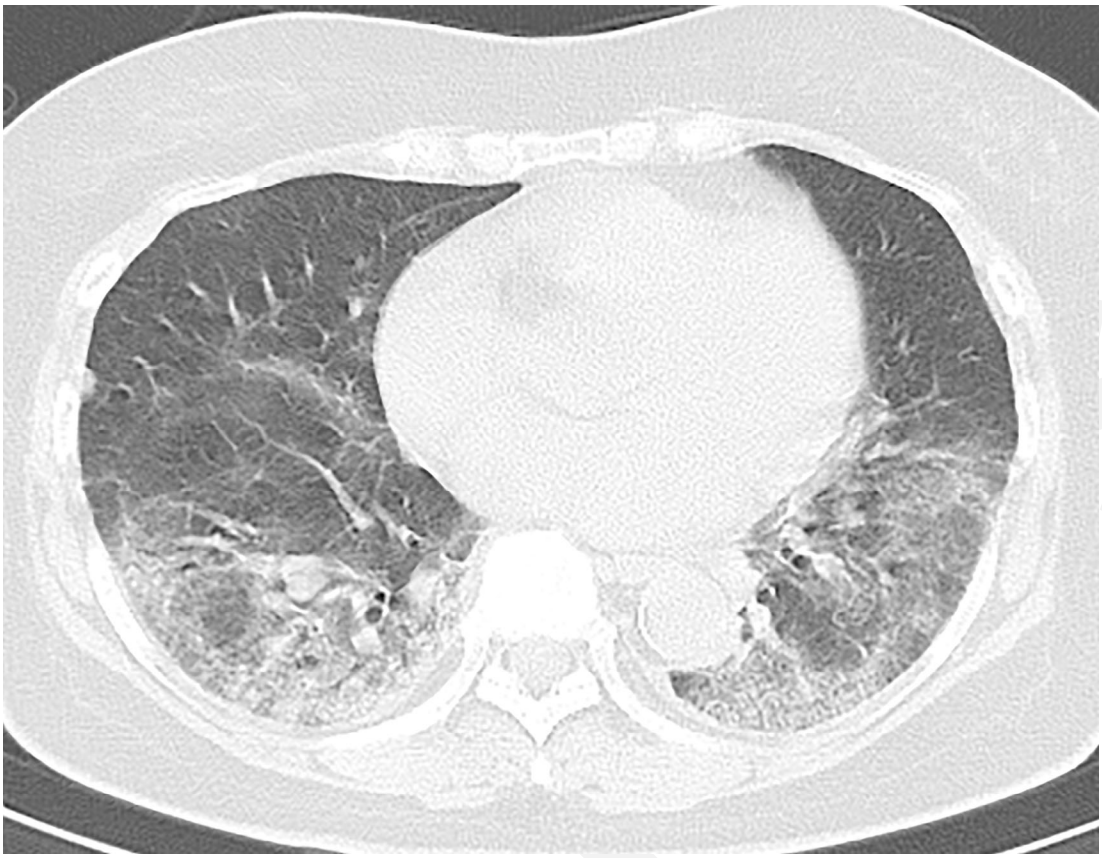

c.

Figure 3. A 73-year-old asymptomatic woman. On axial CT images, focal peripheral ground-glass opacities with intralobular and interlobular smooth septal thickening were shown in the left (a, arrow) and right upper lobe (a, arrowhead). The right upper lobe lesions were accompanied by subpleural curvilinear lines (a, arrow). Diffuse ground-glass (reticular) opacities with consolidation with bronchiectasis and bronchial wall thickening were demonstrated in the left and right lower lobes (b, c).